ornl

OAK
RIDGE
NATIONAL
LABORATORY

UNION
CARBIDE

OPERATED BY
UNION CARBIDE CORPORATION
FOR THE UNITED STATES
DEPARTMENT OF ENERGY

ORNL/TM-7999

Dose Rates from the Induced Activity in the ETF Neutral Beam Injector

R. T. Santoro
J. M. Barnes
R. A. Lillie
R. G. Alsmiller, Jr.

ORNL/TM-7999
Dist. Category UC-20d

Contract No. W-7405-eng-26

Engineering Physics Division

DOSE RATES FROM THE INDUCED ACTIVITY IN THE ETF NEUTRAL BEAM INJECTOR*

R. T. Santoro
J. M. Barnes+
R. A. Lillie
R. G. Alsmiller, Jr.

Date Published - October 1981

*Submitted for
Journal publication

+UCC-ND Computer Sciences Division

This Work Sponsored by
Office of Fusion Energy
U.S. Department of Energy

OAK RIDGE NATIONAL LABORATORY
Oak Ridge, Tennessee 37830
operated by
UNION CARBIDE CORPORATION
FOR THE
DEPARTMENT OF ENERGY

ABSTRACT

The dose equivalent rates outside the Engineering Test Facility neutral beam injector shield from the induced radioactivity have been calculated for the reactor operating at 1140 MW for 1, 30, and 365 days. The dose rates at one day after shutdown are large even after only one day of operation. Depending on the location and operating time, cooling times from 30 d to ∿5 years are required before the dose rates are sufficiently low to allow routine maintenance work in the vicinity of the NBI shield.

I. INTRODUCTION

The Engineering Test Facility (ETF) was envisioned as a beam driven Tokamak reactor and, as such, would employ neutral beam injectors (NBI) to heat and ignite the plasma. Neutral deuterons would be injected into the plasma region through ducts that penetrate the shielding that surrounds the torus. The ~14 MeV neutrons produced from the D-T reactions in the plasma along with the secondary neutrons and gamma rays produced from the interactions of these neutrons in the materials surrounding the plasma will stream through these ducts and cause adverse problems (nuclear heating, radiation damage, and induced activation) that will impact the design, performance, and maintenance of the injectors and other reactor components. In previous papers,[1,2] the calculated results of neutron and gamma ray streaming on the performance of the ETF neutral beam injectors were reported. In Ref. 1, the nuclear heating rate in the NBI cryopumping panels, the dose rate to the ion source insulators, and the biological dose rate as a function of the injection duct concrete shield thickness were reported. In Ref. 2, selected nuclear responses (heating rates, biological dose rates, and reaction rates) were presented in the form of iso-response contours.

In this paper, the biological dose rates from the neutron induced activity of the ETF neutral beam injector are presented. The data were obtained by utilizing the neutron flux distributions in the NBI and injection duct calculated in Ref. 1 as the source term for estimating the spatial dependences of the induced activation. Monte Carlo radiation transport methods were used to calculate the photon transport through the components.

The NBI-injection duct model used in the analysis and the methods of calculation to obtain the dose rates are described in Section II. The results are presented and discussed in Section II.

II. DETAILS OF THE CALCULATIONS

The two-dimensional model of the ETF plasma region, neutral beam injector assembly, and shield used in this study are shown in Fig. 1. The components are modeled in r-z geometry with cylindrical symmetry about the axis of neutral beam injection. The plasma region and the neutral beam injection duct are surrounded by a 1.2-m-thick shield comprised of 65 v/o stainless steel type-316 (SS-316) and 35 v/o water with 6 w/o natural boron added. The NBI is surrounded with 1.0 m of concrete shielding. The components inside of the injector (bending magnet, cryo-pumping panels, calorimeter, baffles, etc.) and the procedures used to represent them in the two-dimensional model of the NBI are discussed in Ref. 3.

The energy and spatial distributions of the neutron and gamma radiation in the ETF and the NBI were calculated using the two-dimensional discrete ordinates code DOT IV.[4] The calculational procedure, described in detail in Ref. 1, consisted of two separate calculations to treat the radiation from two sources: that which streams directly from the plasma into the injector and that which undergoes collisions in the reactor and duct shielding before entering the injector. The first source region was taken to be that volume of the plasma which is viewed from a point on the duct centerline at the entrance to the injector. The radiation originating in this volume was taken to be a point source at the intersection of the

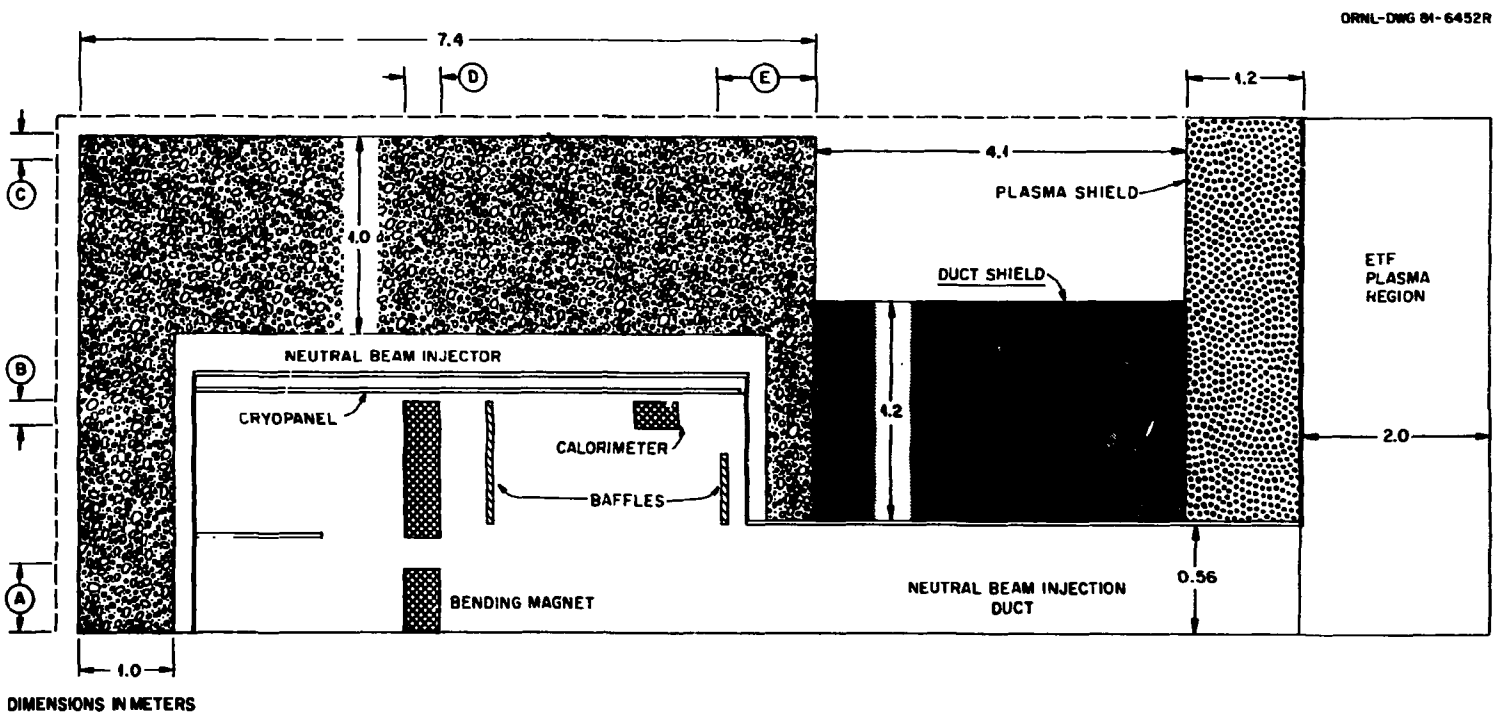

Fig. 1. Two-dimensional representation of the ETF neutral beam injector.

plasma and injector duct centerlines. The second source region is the remaining plasma volume which was approximated using a ring source located at a radial distance of 1.03 m from the intersection of the plasma and duct centerlines. Both source terms include the ~14 MeV neutrons from the D-T reactions in the plasma along with the low energy neutrons and secondary gamma rays that result from the neutron collisions and reactions in the materials that surround the plasma.

For the purpose of this study, only the neutron flux distributions in the geometry mesh used to describe the ETF and NBI are required to calculate the induced activity. The spatial and energy dependent neutron flux obtained from the point (P) and ring (R) sources were combined to form a single distribution. That is

$$\phi(\vec{r},E) = \phi_p(\vec{r},E) + \phi_R(\vec{r},E) \quad . \tag{1}$$

These data were normalized to the case of the ETF operating at 1140 MW.

The neutron flux distributions given by Eq. (1) were used as the input to the MAGIK code system.[5] The production rate of radioactive nuclides of type k at spatial location $\vec{r}$ in the geometry mesh of the NBI and injection duct are obtained from

$$P_k(\vec{r}) = \sum_j n_j(\vec{r}) \int dE \phi(\vec{r},E) \sigma_{jk}(E) \tag{2}$$

where

$n_j(\vec{r})$ = the number of nuclei of type j at $\vec{r}$ and

$\sigma_{jk}(E)$ = the microscopic cross section for the production of a nucleus of type k from the interaction of neutrons having energy E with a nucleus of type j.

These data are used in solving equations of the form

$$D(\vec{r},t) = \sum_k \lambda_k R_k(t) \left\{ \int dE_\gamma C(E_\gamma) \int d\vec{r}' dE_\gamma' P_k(\vec{r}') \Gamma_k(E_\gamma) V(\vec{r},E_\gamma \vec{r}',E_\gamma') \right\} \qquad (3)$$

where

$D(\vec{r},t)$ = the photon dose rate at $\vec{r}$ at time t,

λ_k = the decay constant of nuclei of type k,

$R_k(t)$ = a time factor for nuclei of type k that is proportional to the neutron source strength and the time scenario of a pulsed neutron source,

$C(E_\gamma)$ = photon flux-to-dose conversion factor,

$\Gamma_k(E_\gamma)$ = the number of photons per unit energy per decay emitted at E_γ by nuclei of type k, and

$V(\vec{r},E_\gamma,\vec{r}',E_\gamma')$ = the value function for the photon flux, i.e., the photon flux per unit energy at $\vec{r}$ and E_γ due to one photon per unit time leaving $\vec{r}'$ with energy E_γ'.

The quantity in the bracket in Eq. (3) is time independent and contains all of the information that must be obtained by photon transport calculations. In the work reported here, the term in the bracket was calculated for each k nuclide using the MORSE[6] Monte Carlo code with the ETF, neutral beam injector, and the shielding shown in Fig. 1 represented in cylindrical geometry using the Combinatorial Geometry package in MORSE. The time dependence of the neutron source was introduced and the summation over k was then carried out. In the Monte Carlo calculations, the photon flux per unit energy was determined using a boundary crossing estimator and the dose rates were averaged over the spatial regions shown in Fig. 1.

The activation cross sections were taken primarily from the compilation of D. W. Muir.[7] In those cases where a produced radioactive nucleus has a mestastable state with a half-life that is substantially different from that of the ground state it was arbitrarily assumed that half of the production is to the ground state and half of the production is to the metastable state, since the experimental data giving the production into the separate states are not generally available. This assumption is crude, but since the individual contributions to the dose rates are known at the end of the calculation it is possible to determine if the assumption has any effect on the final results. Residual nuclei with half-lives between 10 min. and 50 years were considered in the calculations. The half-life and photon spectra from each nucleus considered were obtained from the Evaluated Nuclear Structure Data Files that are available from the Nuclear Data Project at the Oak Ridge National Laboratory.[8] The photon transport calculations were performed with the Monte Carlo code MORSE using the cross section data described in Ref. 10. The photon fluxes were converted to dose equivalent rates using the flux-to-dose equivalent rate conversion factors of Claiborne and Trubey.[11]

III. DISCUSSION OF RESULTS

The dose equivalent rates were calculated at spatial locations A-E outside the NBI shield (see Fig. 1) for reactor operating times of 1, 30, and 365 days. A D-T pulse scenario consisting of 200 consecutive pulses of 106 sec duration with 29 sec between pulses was assumed. Each day consists of $\sim$8 hours of D-T operation followed by $\sim$16 hours when the beam is off. This cycle was included in the calculations. The dose

equivalent rates at location A-E as a function of time after shutdown of the reactor are summarized in Table I. The results are normalized to a reactor operating power of 1140 MW which corresponds to a source strength of 1.64×10^{19} particles/sec from the point source and 1.27×10^{20} particles/sec from the ring source.

The dose equivalent rate at one hour after shutdown is large at all locations outside the NBI even after just one day of reactor operation. The dose rates increase as the operating time increases. The dose rates at locations A-D, however, reach a constant level after 30 days of operation. The dose rate at these locations is due mainly to the activated nuclides in concrete and these reach saturation after $\sim$30 days of reactor operation. The dose rate at location E increases continuously with reactor operation. At this location, the dose is due to photons emitted from the concrete NBI shield and from photons emitted from activated nuclei in the SS-316-borated water shield surrounding the injection duct. The radionuclides formed in SS-316 have half-lives much longer than one year and these will not reach saturation until after many years of operation.

The dose rate at locations A-C exhibit a strong dependence on the neutrons streaming from the plasma region. The high dose rate at location A arises from neutrons that stream through the opening in the iron bending magnet and activate the concrete at the rear of the injector. Locations B and C are shielded from the plasma region by the bending magnet and the SS-316-borated water injection duct shield. The dose rate at location D is higher than that at location C principally because of geometric effects; that is, it is closer to the plasma region and the

TABLE I. Dose Equivalent Rate at Various Locations Outside the NBI Vs. Time After the Last Pulse [200 pulses/day, pulse length = 106 s, time between pulses = 29 s; ∿8 h of D-T pulses followed by ∿16 h when the beam is off]

	Dose Equivalent Rate (rem/hr)								
	Time After Shutdown								
Position	1h	8h	1d	30d	180d	1y	2y	5y	10y
	1 Day of Operation								
A	5.45×10^{1}	3.85×10^{1}	1.83×10^{1}	4.84×10^{-4}	1.73×10^{-4}	1.08×10^{-4}	5.58×10^{-5}	1.19×10^{-5}	2.35×10^{-6}
B	1.17×10^{1}	8.43×10^{0}	4.02×10^{0}	1.05×10^{-4}	1.92×10^{-5}	9.52×10^{-6}	6.91×10^{-6}	3.11×10^{-6}	8.22×10^{-7}
C	2.67×10^{-1}	1.93×10^{-1}	9.16×10^{-2}	2.07×10^{-6}	2.07×10^{-7}	2.09×10^{-8}	7.64×10^{-9}	3.42×10^{-9}	9.04×10^{-10}
D	8.99×10^{0}	6.49×10^{0}	3.09×10^{0}	6.51×10^{-5}	8.99×10^{-6}	2.72×10^{-6}	1.28×10^{-6}	2.93×10^{-7}	6.03×10^{-8}
E	3.18×10^{1}	4.40×10^{0}	3.72×10^{0}	2.07×10^{0}	8.43×10^{-1}	4.17×10^{-1}	1.76×10^{-1}	2.87×10^{-2}	8.17×10^{-3}
	30 Days of Operation								
A	8.05×10^{1}	5.74×10^{1}	2.73×10^{1}	1.14×10^{-2}	4.95×10^{-3}	3.16×10^{-3}	1.63×10^{-3}	3.51×10^{-4}	6.98×10^{-5}
B	1.74×10^{1}	1.26×10^{1}	6.00×10^{0}	2.57×10^{-3}	5.20×10^{-4}	2.80×10^{-4}	2.05×10^{-4}	9.23×10^{-5}	2.44×10^{-5}
C	3.97×10^{-1}	2.87×10^{-1}	1.37×10^{-1}	4.95×10^{-5}	5.07×10^{-6}	5.60×10^{-7}	2.27×10^{-7}	1.02×10^{-7}	2.68×10^{-8}
D	1.34×10^{1}	9.68×10^{0}	4.62×10^{0}	1.55×10^{-3}	2.34×10^{-4}	7.79×10^{-5}	3.75×10^{-5}	8.64×10^{-6}	1.79×10^{-6}
E	1.01×10^{2}	7.31×10^{1}	7.14×10^{1}	5.62×10^{1}	2.36×10^{1}	1.20×10^{1}	5.14×10^{0}	8.47×10^{-1}	2.44×10^{-1}
	365 Days of Operation								
A	8.05×10^{1}	5.74×10^{1}	2.73×10^{1}	6.77×10^{-2}	4.15×10^{-2}	2.87×10^{-2}	1.53×10^{-2}	3.59×10^{-3}	7.50×10^{-4}
B	1.74×10^{1}	1.26×10^{1}	6.01×10^{0}	9.61×10^{-3}	3.88×10^{-3}	2.92×10^{-3}	2.22×10^{-3}	9.97×10^{-4}	2.63×10^{-4}
C	3.97×10^{-1}	2.87×10^{-1}	1.37×10^{-1}	1.35×10^{-4}	1.63×10^{-5}	3.89×10^{-6}	2.44×10^{-6}	1.10×10^{-6}	2.90×10^{-7}
D	1.34×10^{1}	9.68×10^{0}	4.62×10^{0}	4.95×10^{-3}	1.26×10^{-3}	6.69×10^{-4}	3.55×10^{-4}	8.90×10^{-5}	1.92×10^{-5}
E	4.10×10^{2}	3.81×10^{2}	3.79×10^{2}	3.21×10^{2}	1.68×10^{2}	9.94×10^{1}	4.60×10^{1}	8.60×10^{0}	2.77×10^{0}

concrete in the vicinity of location D is subjected to a higher neutron flux.

The acceptable dose equivalent rate for workers in radiation fields is 0.10 rem per 40 hour week, or 2.5×10^{-3} rem/hr. Based on this value, access to the rear of the injector is not possible until nearly 30 days after shutdown if the reactor operates for 30 days. If the reactor operates for longer times, the cooling time to reach acceptable dose rate levels increases. At location E, the dose equivalent rate is larger than 2.5×10^{-3} rem/hr for very long times after shutdown (>5 yr) even after one day of operation.

The total dose equivalent rate and the contributions to the total dose equivalent rate from various radionuclides are plotted as a function of time after shutdown following 30 days of reactor operation for locations A-E in Figs. 2-6, respectively. The dose rates at locations A-D, shown in Figs. 2-5, are initially dominated by the photons emitted from ^{24}Na. At times after shutdown greater than $\sim 2 \times 10^{-2}$ y, the dose rate is due to the decay of ^{22}Na and ^{59}Fe. The ^{22}Na and ^{24}Na nuclides are produced as the result of neutron reactions with the sodium in the concrete and ^{59}Fe arises from neutron reactions in the iron reinforcing rods throughout the concrete. The dose rate at location A, shown in Fig. 2, also includes contributions from ^{54}Mn and ^{56}Mn that are produced in the SS-316 NBI enclosure. These nuclides are produced from the neutrons that stream through the opening in the bending magnet and interact in the SS-316.

Shown in Fig. 6 are the radionuclides that contribute to the dose equivalent rate at location E. The dose rate is due mainly to the activation of the SS-316 in the injection duct shield. The ^{56}Mn and ^{58}Co

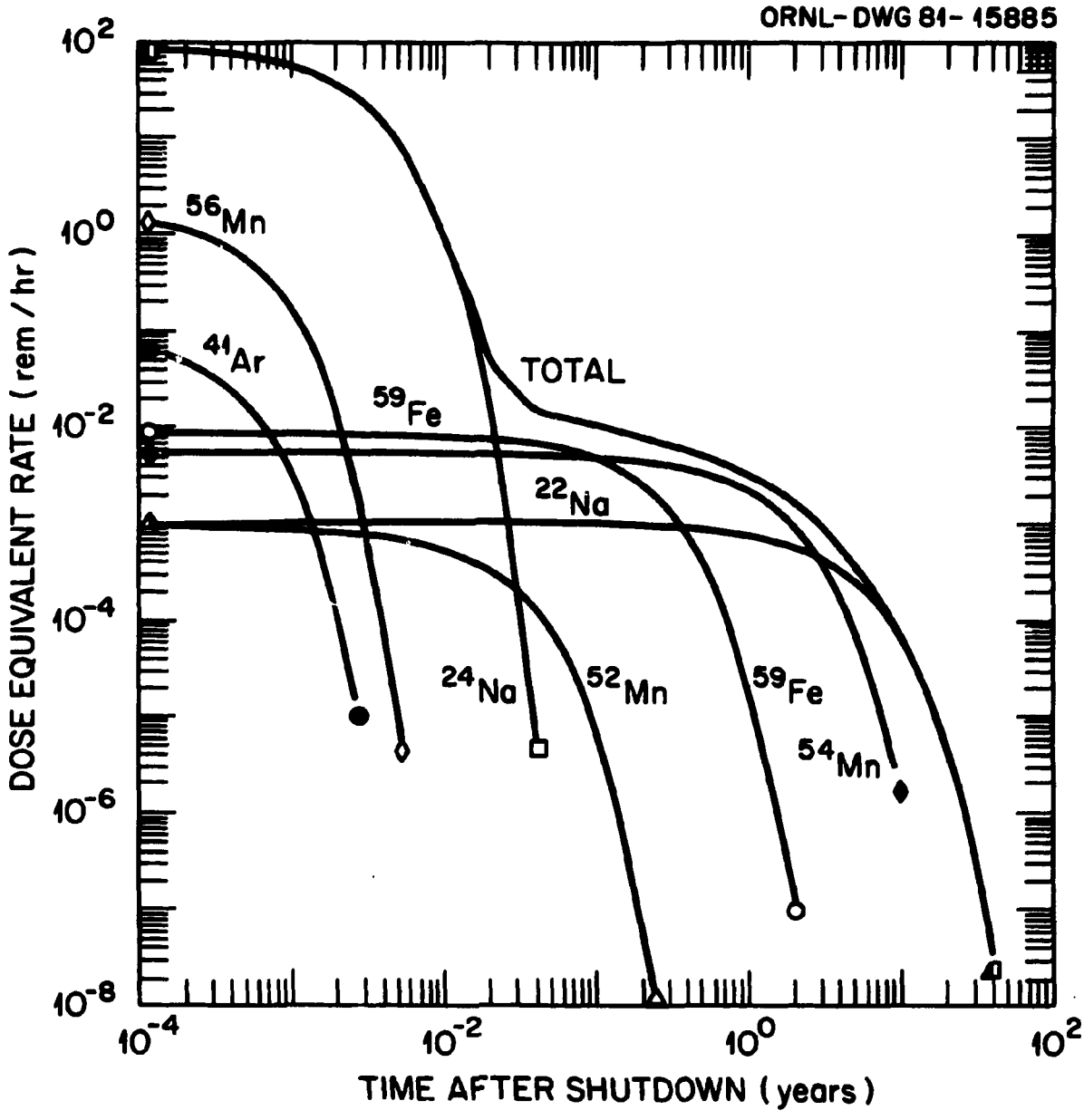

Fig. 2. Dose equivalent rate at location A versus time after shutdown following 30 days of reactor operation.

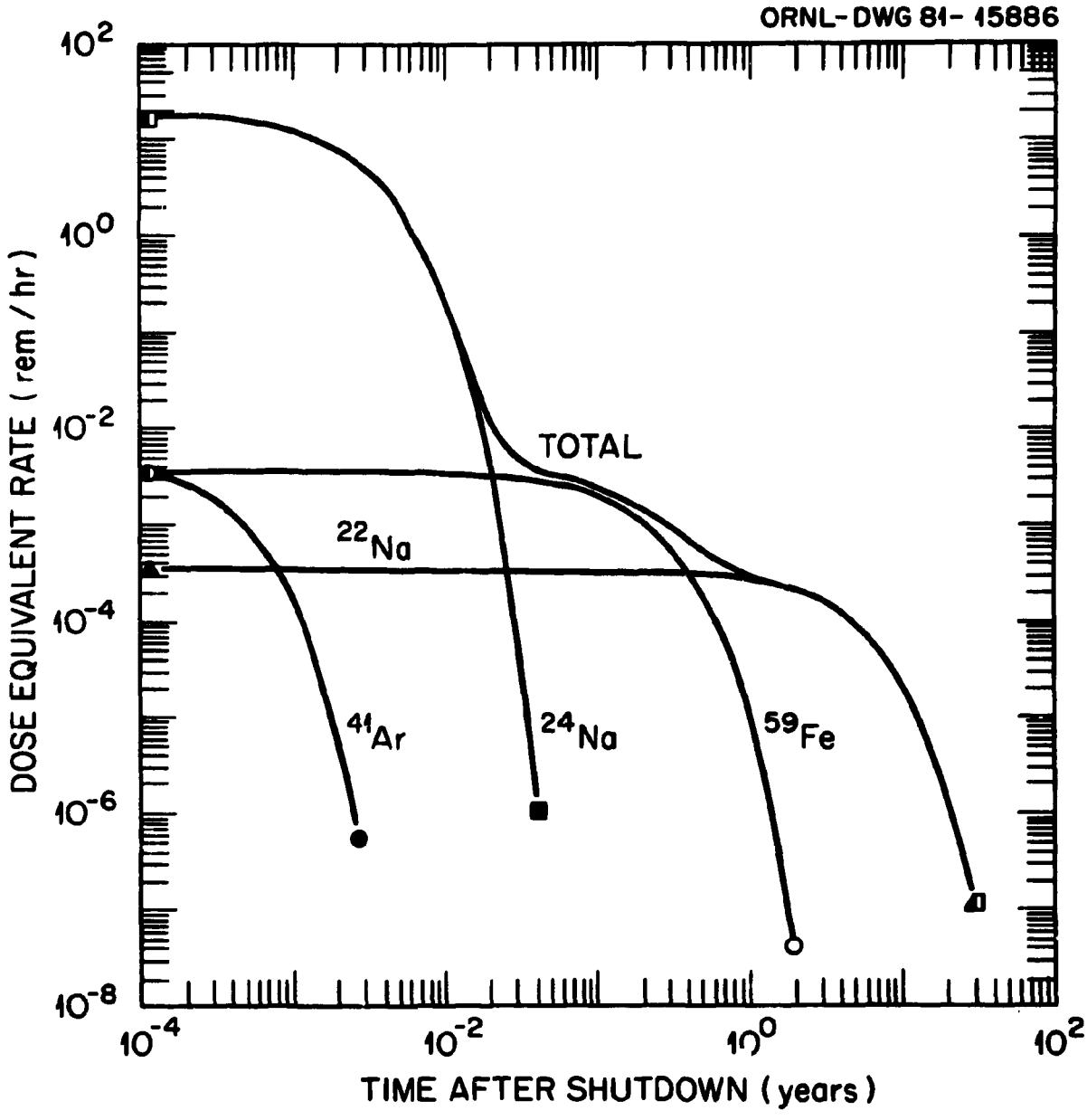

Fig. 3. Dose equivalent rate at location B versus time after shutdown following 30 days of reactor operation.

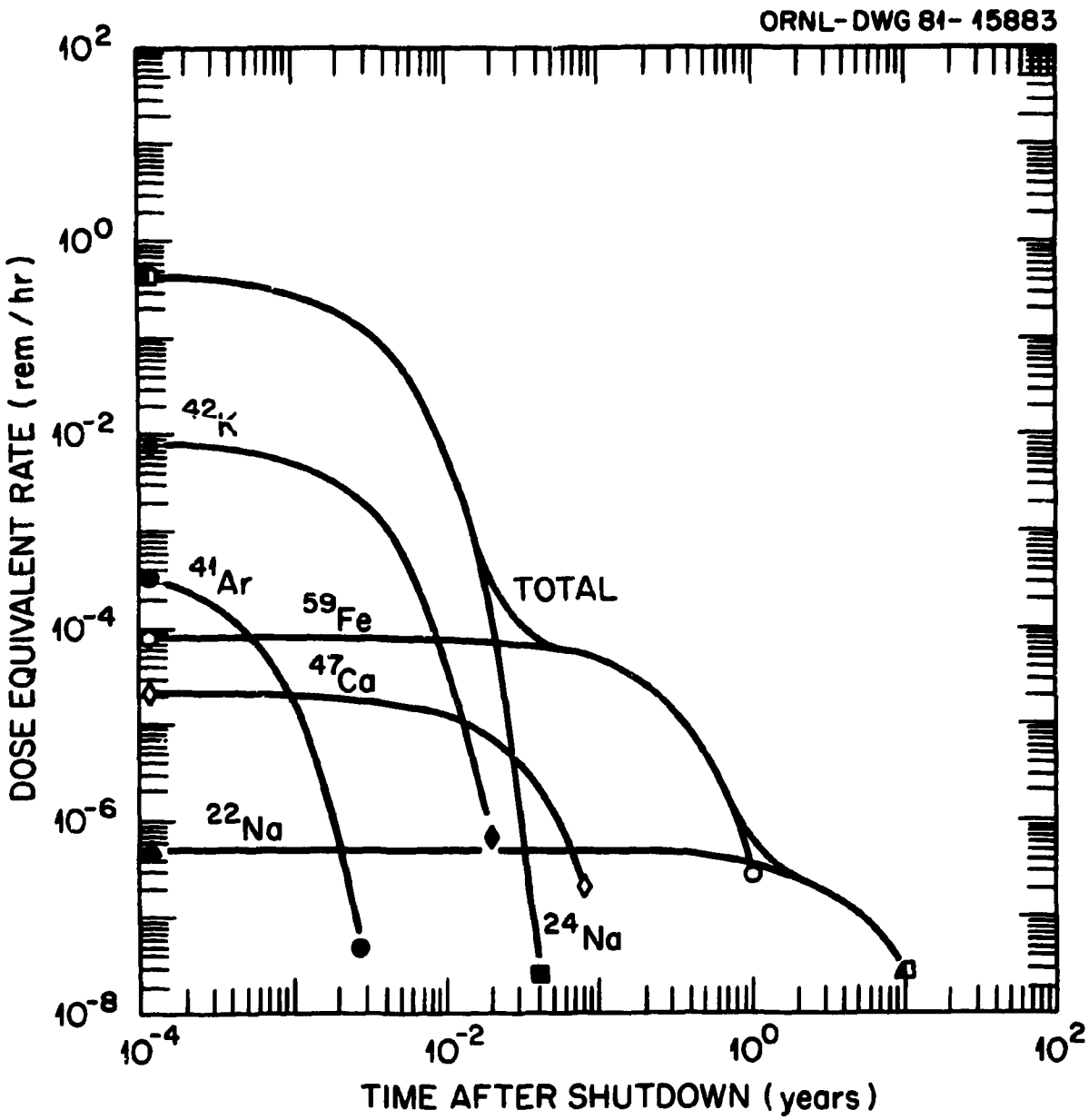

Fig. 4. *Dose equivalent rate at location C versus time after* shutdown following 30 days of reactor operation.

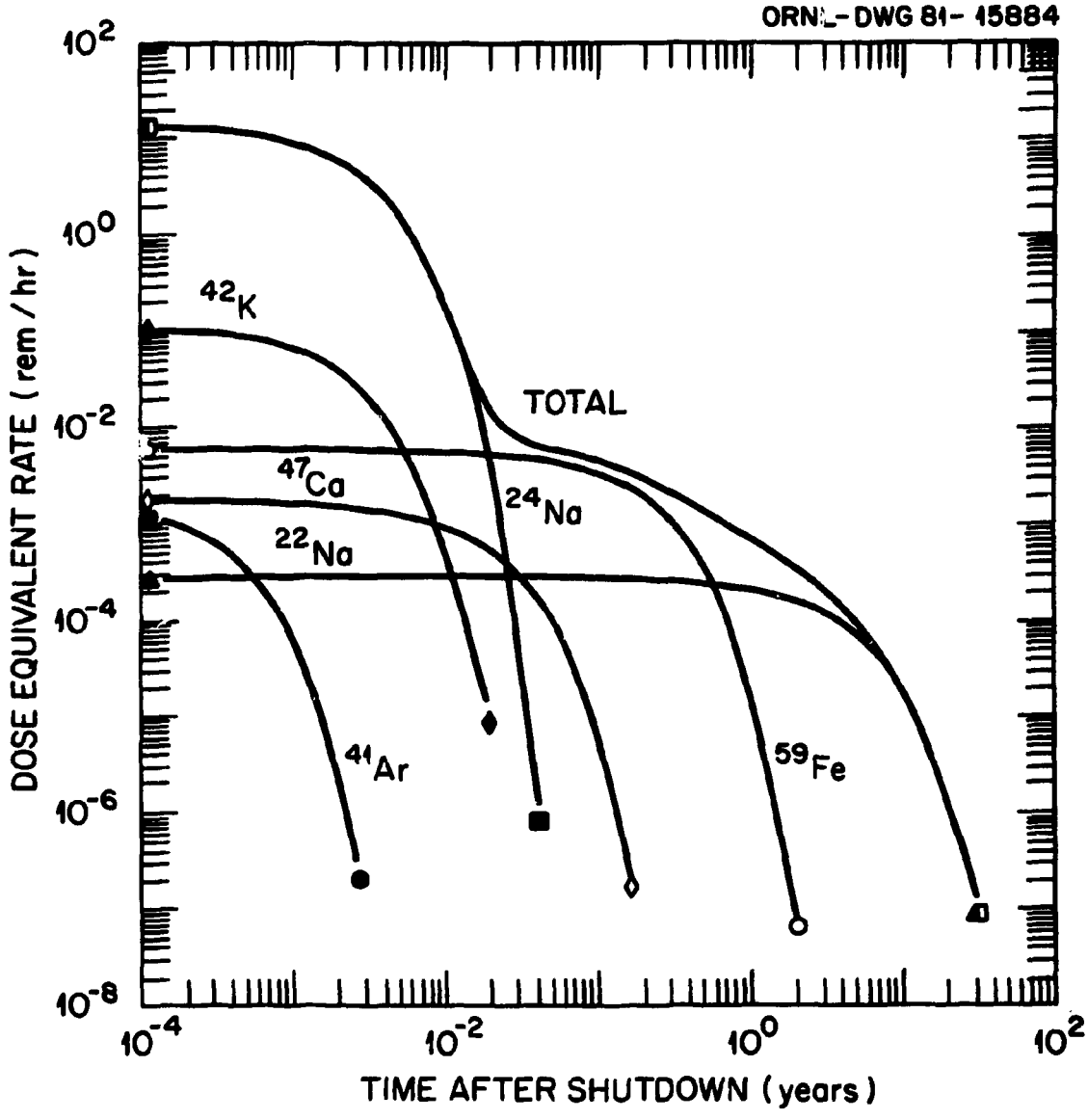

Fig. 5. Dose equivalent rate at location D versus time after shutdown following 30 days of reactor operation.

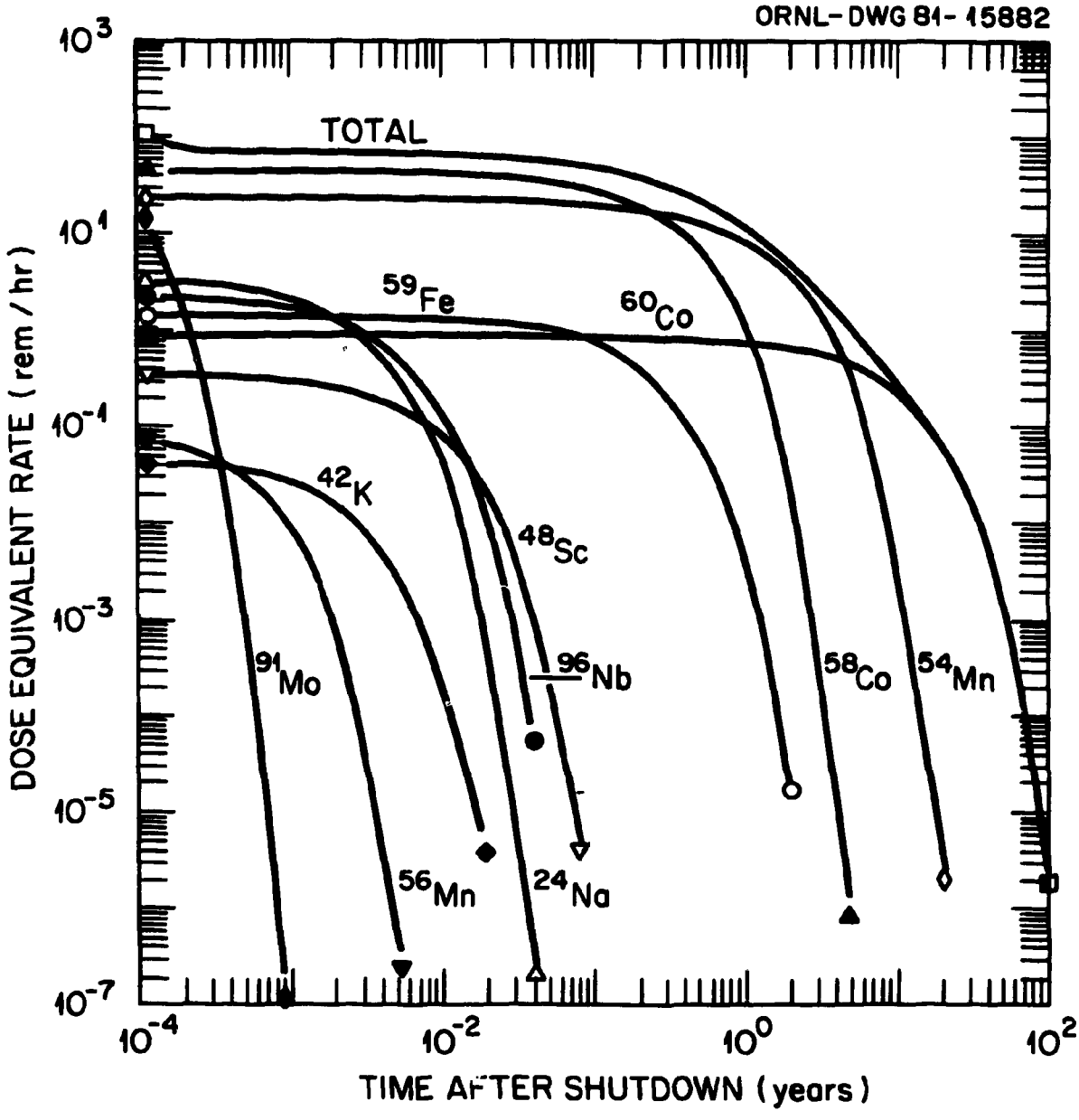

Fig. 6. Dose equivalent rate at location E versus time aft shutdown following 30 days of reactor operation.

radionuclides dominate the dose rate for times after shutdown longer than ∿5 years.

REFERENCES

1. R. A. Lillie, R. T. Santoro, R. G. Alsmiller, Jr., J. M. Barnes "Neutron and Gamma Ray Streaming Calculations for the ETF Neutral Beam Injectors," ORNL/TM-7705, Oak Ridge National Laboratory (1981).

2. J. M. Barnes, R. T. Santoro, R. A. Lillie, R. G. Alsmiller, Jr., "Iso-Response Contours in the ETF Neutral Beam Injectors," ORNL/TM-7783, Oak Ridge National Laboratory (1981).

3. R. T. Santoro, R. A. Lillie, R. G. Alsmiller, Jr., J. M. Barnes, Nucl. Sci. Eng. 60, 225 (1979).

4. W. A. Rhoades, D. B. Simpson, R. L. Childs and W. W. Engle, Jr., "The DOT 1V Two-Dimensional Discrete Ordinates Code with Space Dependent Mesh and Quadrature," ORNL/TM-6529, Oak Ridge National Laboratory (1979).

5. J. Barish, T. A. Gabriel and R. G. Alsmiller, Jr., "MAGIK - A Monte Carlo System for Computing Induced Residual Activity Dose Rates," ORNL-5561, Oak Ridge National Laboratory (1979).

6. M. B. Emmett, "The MORSE Monte Carlo Radiation Transport System," ORNL-4972, Oak Ridge National Laboratory (1975).

7. D. W. Muir, "DLC-33 Data Library MONTAGE," Radiation Shielding Information Center, Oak Ridge National Laboratory (1975).

8. H. C. Claiborne and D. K. Trubey, "Nucl. Appl. Technol. 8, 450 (1970).